Halo and Pionless Effective Field Theories for Describing Nuclear Structures and Reactions

Chen Ji

Central China Normal University

EFB25 Mainz, Germany
2023.08.03

Nucleosynthesis & astrophysical processes

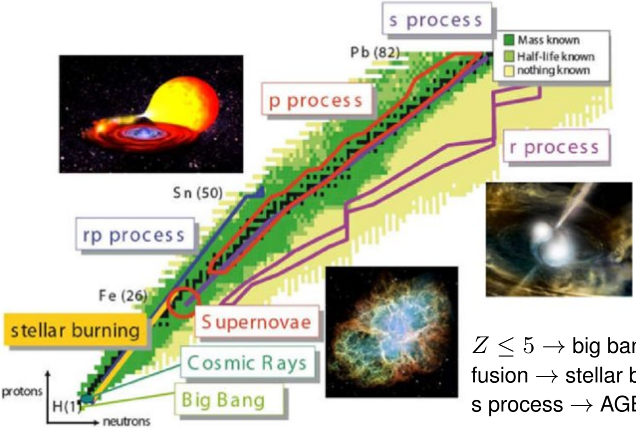

118 known elements

∼3000 known isotopes

∼4000 unknown isotopes

$Z \leq 5 \rightarrow$ big bang / cosmic ray

fusion $\rightarrow$ stellar burning

s process $\rightarrow$ AGB star

r process $\rightarrow$ supernovae & neutron-star merger

p & rp process $\rightarrow$ sun-neutron-star binary

pic: Senger, Particles 3 (2020) 320

Halo nuclei

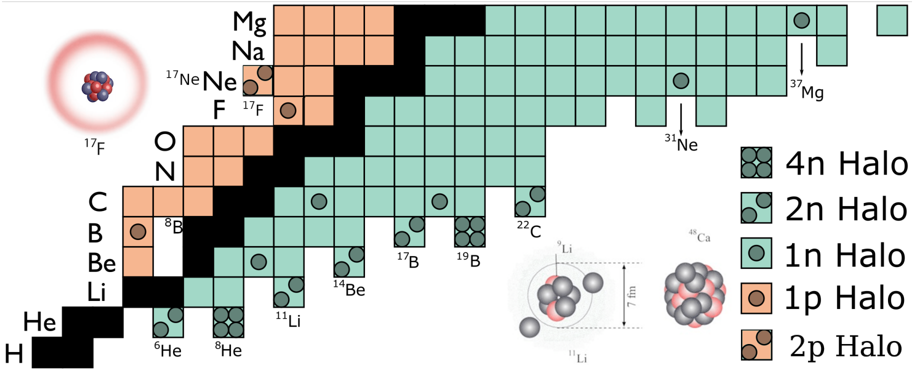

- far from stability (close to drip line)
- exhibit unique quantum features
  - light, p-rich or n-rich
  - bound/resonant states close to breakup threshold
- cluster structures
  - tight core surrounded loosely by valence nucleon(s)
  - large spatial extent
- enhanced cross section in astrophysical reaction at finite temperature

Halo nuclei challenge nuclear theories

- Phases of halo theories
  - Back-of-the-envelope period
    - "quick and dirty" estimates of halo properties by reproducing σ_R
    - gaussian spatial distribution $\rightarrow$ reproduce $\sigma_I \rightarrow R_m$ too small!
  - Few-body models period
    - cluster structure models (core + valence nucleons)
    - few-body reaction models (Glauber, DWBA, CDCC,...)
    - unresolved model dependence
    - limited applicable regimes
  - Microscopic models period
    - ab initio structure theory
    - difficulties in computational power & extension to threshold physics
    - need to develop ab initio reaction theory (e.g. optical potential)

Halo Nuclei, Al-Khalili, Morgan & Claypool Publishers, 2017

  - Effective field theory
    - systematically embed microscopic information in cluster model
    - provide guidance to build reaction theory

NN interaction in atomic nuclei

QCD

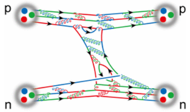

$\Lambda \sim 1\text{GeV}$

$Q \sim 100$ MeV

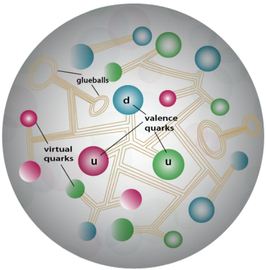

Λ: EFT breakdown scale

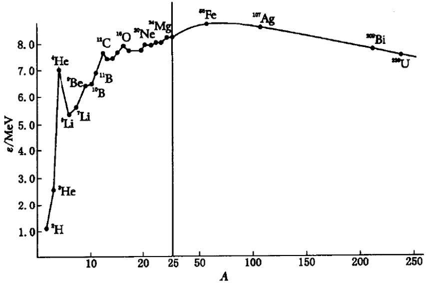

$Q \approx \sqrt{2M_N B/A}$: typical scale in EFT

NN interaction in atomic nuclei

QCD

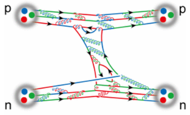

$\Lambda \sim 1$GeV

$Q \sim 100$ MeV

phenomenology

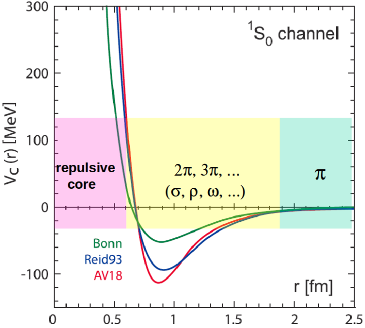

pic: Aoki et al. Comp. Sci. Disc. 2008

NN interaction in atomic nuclei

QCD

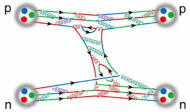

$\Lambda \sim 1\text{GeV}$

$Q \sim 100$ MeV

phenomenology

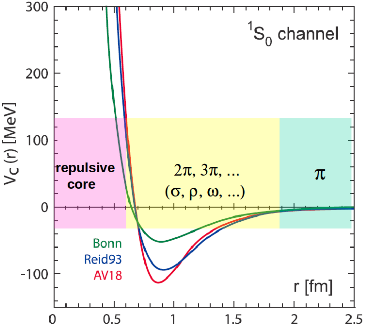

pic: Aoki et al. Comp. Sci. Disc. 2008

chiral EFT

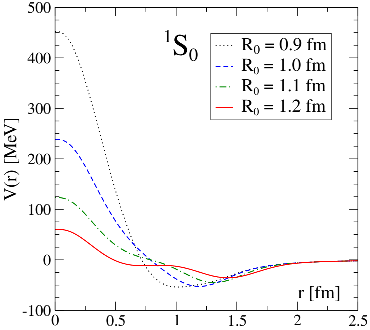

pic: Gezerlis et al. Phys. Rev. C 2014

EFT with contact interactions

- Effective field theory with contact interactions originate from pionless EFT

chiral EFT NN force

- short range: $V_s = C_0$
- intermediate/long range:

$$V_{1\pi} \sim \frac{1}{q^2 + m_\pi^2}$$

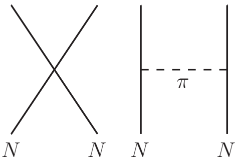

EFT with contact interactions

- Effective field theory with contact interactions originate from pionless EFT

chiral EFT NN force

- short range: $V_s = C_0$
- intermediate/long range:

$$V_{1\pi} \sim \frac{1}{q^2 + m_\pi^2}$$

$\not\pi$EFT NN force

- NN momentum $q^2 \ll m_\pi^2$

$$V_{1\pi} \xrightarrow{q^2 \ll m_\pi^2} C_0 + C_2 q^2 + \cdots$$

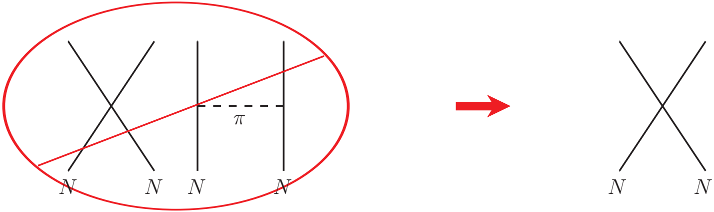

Universality in $\not{\pi}$EFT

Phillips Line: a_{nd} vs $B(^3\mathrm{H})$

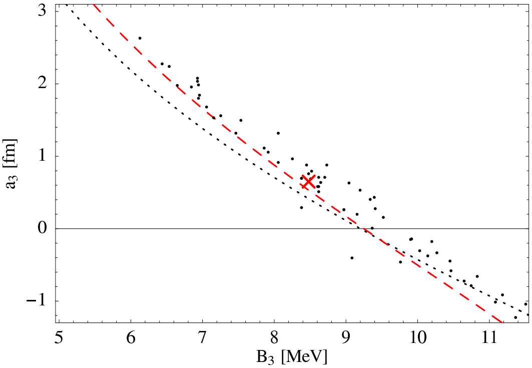

Tjon Line: $B(^3\mathrm{H})$ vs $B(^4\mathrm{He})$

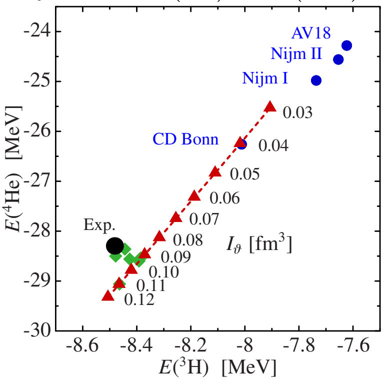

- $\not{\pi}$EFT indicates universal correlations among few-body observables
- long-range (low-energy) physics is insensitive to details of short-range interactions

Nuclear halo and cluster

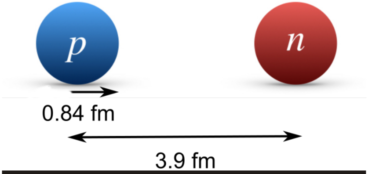

few-body molecular structure

- ^{2}H
  - simplest neutron halo
- neutron halos
  - ^{6}He, ^{11}Be, . . .
- proton halos
  - ^{17}F*, ^{8}B
- α-clustering
  - ^{9}Be: $\alpha + \alpha + n$
  - ^{8}Be, ^{12}C*

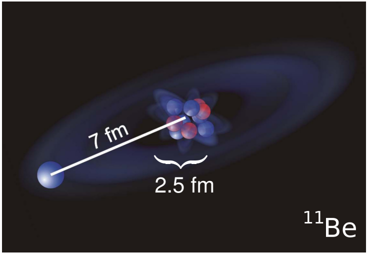

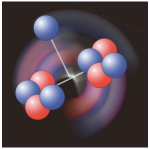

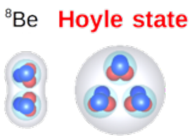

Halo physics near clustering threshold

ab initio theory

$\Lambda \sim \sqrt{m_N E^*_{\text{core}}}$

$Q \sim \sqrt{m_N S_N}$

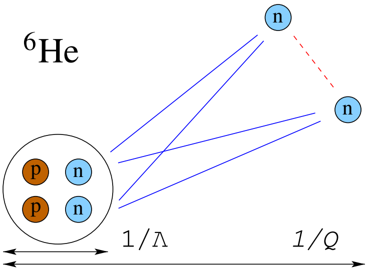

Halo physics near clustering threshold

ab initio theory

$\Lambda \sim \sqrt{m_N E^*_{\rm core}}$

$Q \sim \sqrt{m_N S_N}$

halo physics is difficult for ab initio theories

- continuum problem in many-body calculations
  NCSMC, GSM-Bergren, Lattice-EFT, LIT, $\cdots$
- uncertainty control in chiral potentials
  threshold observable converges slower in χEFT

$$\text{halo scale}: Q_{\rm halo} \ll Q_{\chi\rm EFT} \approx (2M_N B/A)^{1/2}$$

$$\text{uncertainty}: \ \Delta_{\rm halo}\% \approx \frac{Q_{\chi\rm EFT}}{Q_{\rm halo}} \left(\frac{Q_{\chi\rm EFT}}{\Lambda_{\chi\rm EFT}}\right)^{(n+1)}$$

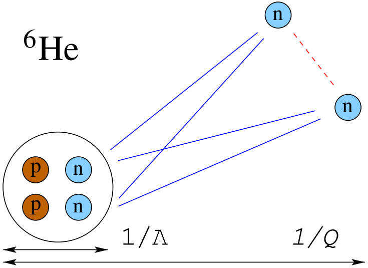

ab initio description of halo features

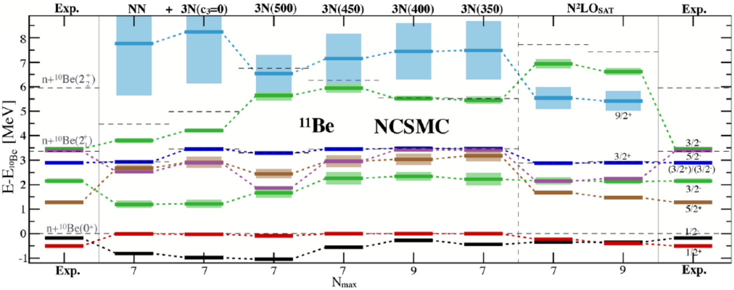

FIG. 2. NCSMC spectrum of ^{11}Be with respect to the $n + {}^{10}$Be threshold. Dashed black lines indicate the energies of the ^{10}Be states. Light boxes indicate resonance widths. Experimental energies are taken from Refs. [1,51].

- ab initio calculation of ^{11}Be has been done by NCSMC
- predictions of threshold properties rely significantly on the nuclear interactions

Calci et al. Phys. Rev. Lett. 117 (2016) 242501

Halo physics near clustering threshold

ab initio theory

$\Lambda \sim \sqrt{m_N E^*_{\rm core}}$

$Q \sim \sqrt{m_N S_N}$

cluster model

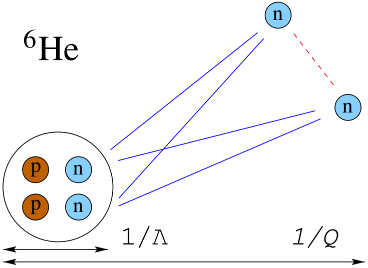

difficulties in cluster models:

- assess model dependence?
- assign theory uncertainty

Halo physics near clustering threshold

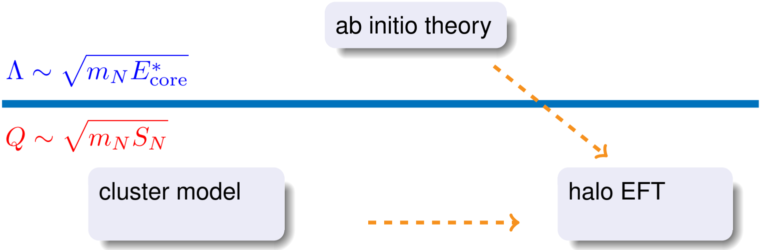

- cluster configuration in halo EFT:
  core + valence nucleons d.o.f.
- separation of scales:
  $Q \ll \Lambda \rightarrow$ systematic expansion in observables
- short-range physics from underlying theory:
  anti-symmetrization of core nucleons is embedded in contact interactions

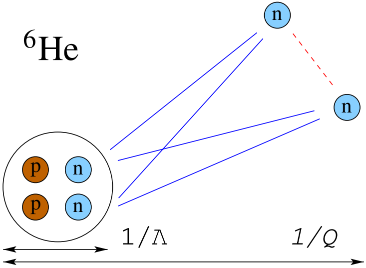

Halo Effective Field Theory

- We adopt EFT with <u>contact interactions</u> to describe clustering in halo nuclei
- introduce auxiliary two-body fields for bound/resonance states

$$
\begin{aligned}
\mathscr{L} &= \mathscr{L}_1 + \mathscr{L}_2 + \mathscr{L}_3 \\
\mathscr{L}_1 &= n^\dagger\left(i\partial_0 + \frac{\nabla^2}{2m_n}\right)n + c^\dagger\left(i\partial_0 + \frac{\nabla^2}{2m_c}\right)c \\
\mathscr{L}_2 &= s^\dagger\left[\eta_0\left(i\partial_0 + \frac{\nabla^2}{4m_n}\right) + \Delta_0\right]s + \sigma^\dagger\left[\eta_1\left(i\partial_0 + \frac{\nabla^2}{2(m_n+m_c)}\right) + \Delta_1\right]\sigma \\
&\quad + g_0\left[s^\dagger(nn) + \text{h.c.}\right] + g_1\left[\sigma^\dagger(nc) + \text{h.c.}\right], \\
\mathscr{L}_3 &= h\,(\sigma n)^\dagger(\sigma n)
\end{aligned}
$$

- 2-body contact (LO)

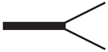

$= -i\sqrt{2}g$

$g \leftarrow$ 2-body observable

- 3-body contact (LO)

$= ih$

$h \leftarrow$ 3-body observable

One-neutron s-wave halos

	^{2}H	^{11}Be	^{15}C	^{19}C
Experiment				
S_{1n} [MeV]	2.224573(2)	0.50164(25)	1.2181(8)	0.58(9)
E_c^* [MeV]	140	3.36803(3)	6.0938(2)	1.62(2)
$\langle r_{nc}^2 \rangle^{1/2}$ [fm]	3.936(12)	6.05(23)	4.15(50)	6.6(5)
	3.95014(156)	5.7(4)	7.2±4.0	6.8(7)
		5.77(16)	4.5(5)	5.8(3)
Halo EFT				
Q/Λ	0.33	0.39	0.45	0.6
r_0/a_0	0.32	0.32	0.43	0.33
$\sqrt{\mathcal{Z}_R}$	1.295	1.3	1.63	1.3
$\langle r_{nc}^2 \rangle^{1/2}$ [fm]	3.954	6.85	4.93	5.72

Electric form factor $\rightarrow$ radius $\langle r_{nc}^2 \rangle^{1/2}$

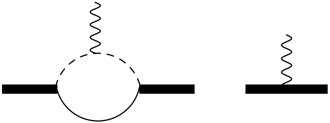

$$F_{nc}(q^2) = \mathcal{Z}_R \frac{2\gamma_0}{q} \arctan\left(\frac{q}{2\gamma_0}\right) + 1 - \mathcal{Z}_R$$

$$F_{nc}(q^2) = 1 - \frac{1}{6}\langle r_{nc}^2 \rangle q^2 + \mathcal{O}(q^4),$$

Coulomb dissociation in $1n$ halos

- Coulomb dissociation
  - breakup by colliding a halo nucleus with a high-Z nucleus
  - the halo dynamics dominates when $E_\gamma \sim S_{1n}$

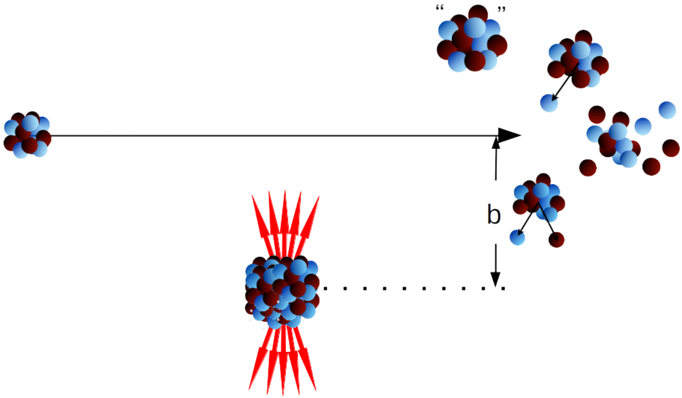

EFT on Coulomb dissociation

- **E1 transition**

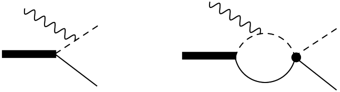

$$\frac{dB(E1)}{dE_\gamma} = \frac{1}{(2\pi)^3}\left(|\mathcal{M}_{E1}^{(J=1/2)}|^2 + |\mathcal{M}_{E1}^{(J=3/2)}|^2\right)\frac{d^3p}{dE_\gamma} = \frac{\mathcal{Z}_R Q_{\rm eff}^2}{\mu_{nc} S_{1n}^2}\frac{3\alpha_{em}}{\pi^2}\frac{(E_\gamma/S_{1n})^{3/2}}{(E_\gamma/S_{1n}+1)^4}.$$

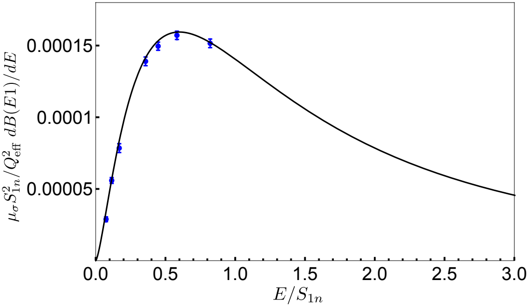

deuteron E1 strength

Hammer, CJ, Phillips, JPG 44 (2017) 103002

EFT on Coulomb dissociation

- **E1 transition**

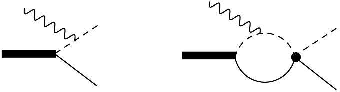

$$\frac{d\sigma}{dE_\gamma} = \frac{16\pi^3}{9} N_{E1}(E_\gamma, R) \qquad \frac{d\mathrm{B(E1)}}{dE_\gamma}$$

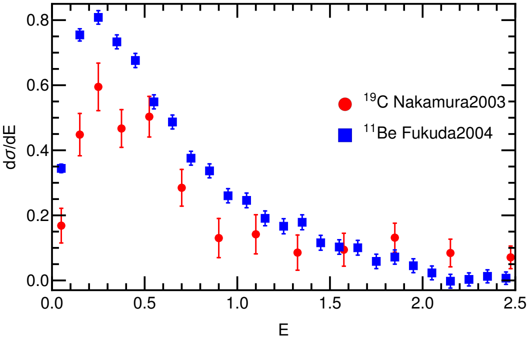

Coulomb dissociation energy spectrum in ^{11}Be and ^{19}C

EFT on Coulomb dissociation

- **E1 transition**

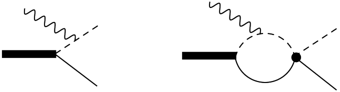

$$\frac{\mu_{nc} S_{1n}^2}{\mathcal{Z}_R Q_{\rm eff}^2}\frac{d\sigma}{dE_\gamma} = \frac{16\pi^3}{9} N_{E1}(E_\gamma, R)\frac{\mu_{nc} S_{1n}^2}{\mathcal{Z}_R Q_{\rm eff}^2}\frac{d\mathrm{B(E1)}}{dE_\gamma}$$

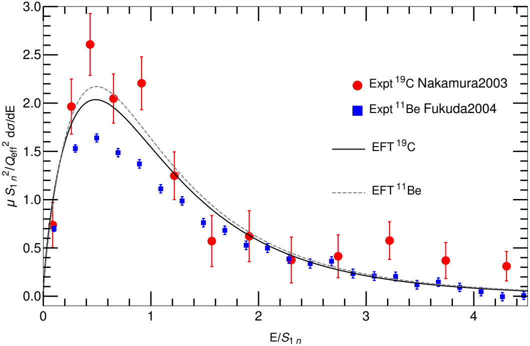

Coulomb dissociation energy spectrum in ^{11}Be and ^{19}C $\rightarrow$ Universality!
^{11}Be: fit ANC in NCSMC [Calci *et al.* '16]

Hammer, Phillips, NPA '11
Acharya, Phillips, NPA '13
Hammer, CJ, Phillips, JPG '17

^{6}He: $2n$ Halo with p-wave nc interactions

- *ab intio* **calculation**
  - no-core shell model Navrátil *et al.* '01; Sääf, Forssén '14
  - NCSM-RGM/Continuum Romero *et al.* '14 '16
  - Green's function Monte Carlo Pieper *et al.* '01; '08
  - hyperspherical harmonics (EIHH) Bacca *et al.* '12

- **Halo EFT in ^{6}He ground state**
  - EFT+Gamow shell model (GSM) Rotureau, van Kolck Few Body Syst. '13
  - EFT+Faddeev equation C.J., Elster, Phillips, PRC '14;

    Göbel, Hammer, CJ, Phillips, Few Body Syst. 60 (2019) 61

- $^{6-10}$He effective interaction + GSM Fossez, Rotureau, Nazarewicz, PRC '18

P-wave neutron halos

- nc interaction in a p-wave bound/resonance state

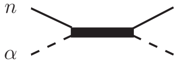

$$= \frac{2\pi}{\mu} \frac{\vec{p} \cdot \vec{q}}{-1/a_1 + r_1 k^2/2 - ik^3}$$

  - $a_1 < 0$: shallow resonance: ^{5}He $(3/2^-)$
  - $a_1 > 0$: shallow bound state: ^{11}Be $(1/2^-)$, ^{8}Li (2^+), ^{8}Li* (1^+)

- p-wave power counting
  - resum ik^3: $1/a_1 \sim Q^3$, $r_1 \sim Q$ [Bertulani, Hammer, van Kolck NPA '02]
  - perturbative ik^3: $1/a_1 \sim Q^2\Lambda$, $r_1 \sim \Lambda$ [Bedaque, Hammer, van Kolck PLB '03]

$2n$ halos in Faddeev formalism

- **solving transition amplitudes $\mathcal{A}_c$ and $\mathcal{A}_n$**

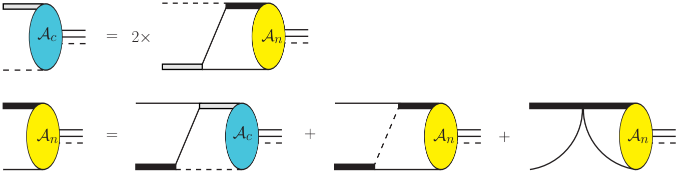

C.J., Elster, Phillips, PRC ’14;
Hammer, CJ, Phillips, JPG ’17

$2n$ halos in Faddeev formalism

- **solving transition amplitudes $\mathcal{A}_c$ and $\mathcal{A}_n$**

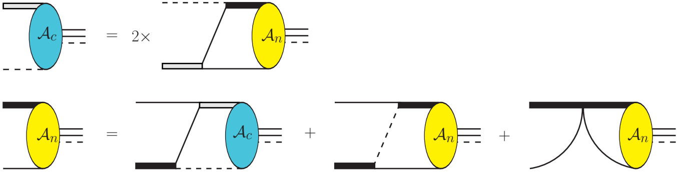

- **three-body wave functions**

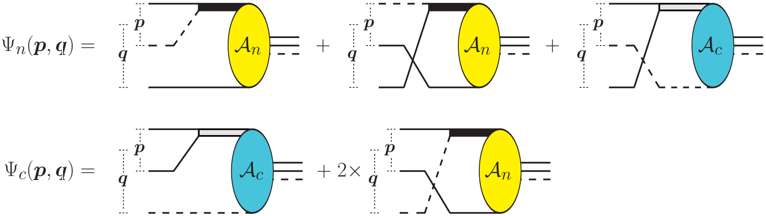

C.J., Elster, Phillips, PRC ’14;

Hammer, CJ, Phillips, JPG ’17

Momentum-space probability density

- completeness in energy-dependent hamiltonian

$$1 = \sum_\alpha |\psi_\alpha\rangle\langle\langle\psi_\alpha| = \sum_\alpha |\psi_\alpha\rangle\langle\psi_\alpha|D^{-1}$$

$$\langle\psi_\alpha|D^{-1} \approx \langle\psi_\alpha|\sqrt{1 - V'(E_\alpha)}$$

- The probability density:

$$\rho_i(\boldsymbol{p},\boldsymbol{q}) = {}_i\langle\boldsymbol{p},\boldsymbol{q}|\Psi\rangle$$

$$\left[\langle\Psi|\boldsymbol{p},\boldsymbol{q}\rangle_i - \mathrm{Re}\sum_j \langle\Psi|V_j'(E_\alpha - \frac{q_j^2}{2\mu_{j(ki)}})|\boldsymbol{p},\boldsymbol{q}\rangle_i\right]$$

- ℓth moment (partial-wave decomposition)

$$\rho_i^{(l)}(p,q) = \int_{-1}^{1} d(\hat{p}\cdot\hat{q})\, P_\ell(\hat{p}\cdot\hat{q})\rho_i(\boldsymbol{p},\boldsymbol{q})$$

- $\rho_n^{(0)}(p,q)$ and $\rho_n^{(1)}(p,q)$

Göbel, Hammer, CJ, Phillips, Few Body Syst. 60 (2019) 61

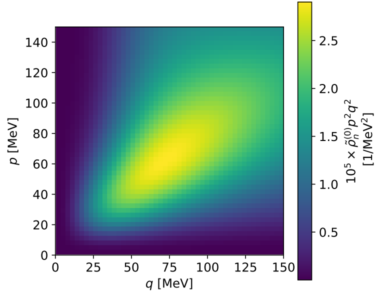

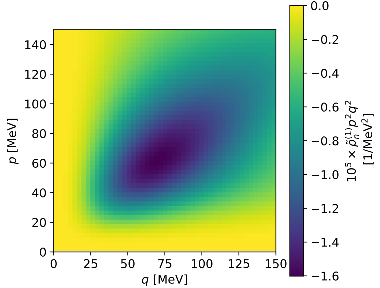

Unconventional momentum-dependent $n\alpha$ interaction

- If $a_0 \sim r_0 \sim Q^{-1}$ in s-wave interaction, we need to tune both a_0 and r_0 at LO

$$V_0(p,p') = -\frac{2\pi}{\mu}\frac{\lambda}{\sqrt{p'^2+2\mu\Delta}\sqrt{p^2+2\mu\Delta}}$$

Peng, Lyu, König, Long (2021), PRC 105, 054002 (2022); Beane, Farrell, FBS 63, 45 (2022); van Kolck, Symmetry 14, 1884 (2022)

- For $n\alpha$ p-wave interaction, both a_1 and r_1 are at LO

$$V_1(p,p') = -\frac{2\pi}{\mu}\frac{\lambda p p'}{\sqrt{p'^2+2\mu\Delta}\sqrt{p^2+2\mu\Delta}}$$

- on-shell t-matrix:

$$T^{(0)}(k,k;k) = -\frac{2\pi}{\mu}\frac{k^2}{-\frac{1}{a_1}+\frac{1}{2}r_1 k^2 - ik^3} \qquad V(E): k^2 \to pp'$$

$$\to \text{resonance} + \text{spurious pole}$$

- off-shell t-matrix:

$$T_1(p',p;k) = -\frac{2\pi}{\mu}\frac{p'}{\sqrt{p'^2+\gamma^2}}\frac{ik-\gamma}{k^2+i(\gamma+\frac{r_1}{2})k+\frac{1}{a_1\gamma}}\frac{p}{\sqrt{p^2+\gamma^2}}$$

$$\gamma + \frac{r_1}{2} + a_1^{-1}\gamma^{-2} = 0 \qquad \text{spurious pole vanishes}$$

Li, Lyu, CJ, Long, arXiv:2303.17292 (accepted at PRC)

Unconventional $n\alpha$ interaction in ^{6}He

- Implementing unconventional p-wave potential in $nn\alpha$ system
- Running of $H(\Lambda)$ and $B(\Lambda)$

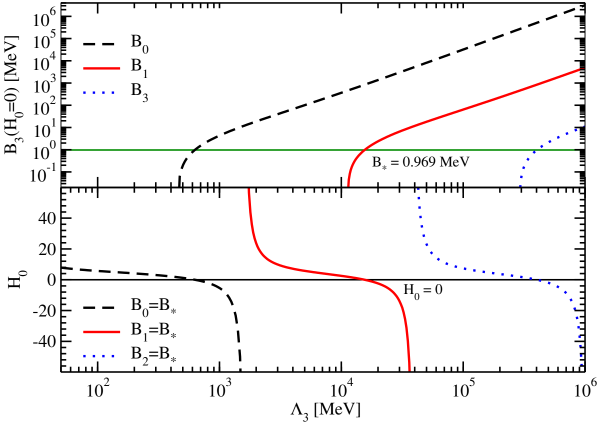

Li, Lyu, CJ, Long, arXiv:2303.17292 (accepted at PRC)

Unconventional $n\alpha$ interaction in ^{6}He

- Implementing unconventional p-wave potential in $nn\alpha$ system
- Running of $H(\Lambda)$ and $B(\Lambda)$
- Faster cutoff convergence of Faddeev components with unconventional potential

energy-dependent $n\alpha$ interaction

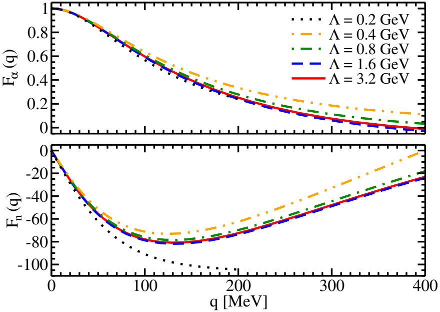

unconventional $n\alpha$ interaction

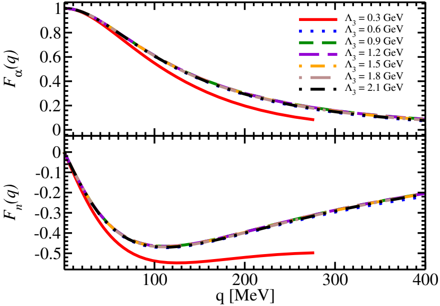

Li, Lyu, CJ, Long, arXiv:2303.17292 (accepted at PRC)

Universal Correlations Among Radii & S_{2n} in ^{6}He

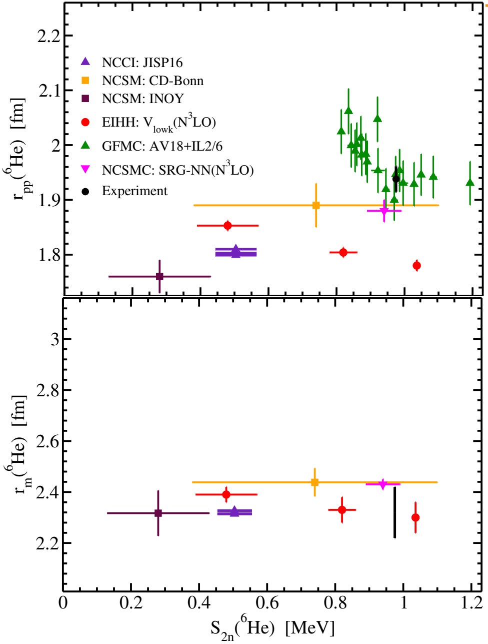

- **He-6 charge radius**
- **He-6 matter radius**

compare with ab initio calculations

NCCI: Caprio, Maris, Vary, PRC '14

NCSM: Caurier, Navratil, PRC '06

EIHH: Bacca, Barnea, Schwenk, PRC '12

GFMC: Pieper, RNC '08

NCSMC: Romero et al., PRL '16

Halo EFT: preliminary (uncertainty)

Universal Correlations Among Radii & S_{2n} in ^{6}He

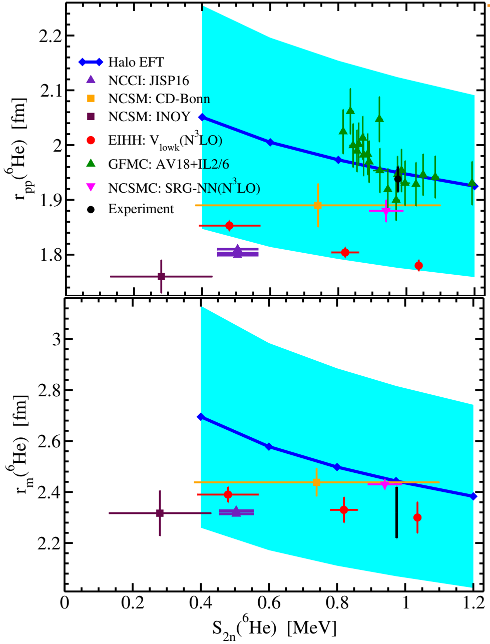

- **He-6 charge radius**
- **He-6 matter radius**

compare with ab initio calculations

NCCI: Caprio, Maris, Vary, PRC ’14

NCSM: Caurier, Navratil, PRC ’06

EIHH: Bacca, Barnea, Schwenk, PRC ’12

GFMC: Pieper, RNC ’08

NCSMC: Romero et al., PRL ’16

Halo EFT: preliminary (uncertainty)

α-clustering in nuclei

- ^{9}Be $\alpha - \alpha - n$ Borromean structure
  - Formation of ^{9}Be strongly influences r-process nucleosynthesis in neutron-rich environment
  - α-clustering drives ^{9}Be's fusion mechanism:

    sequential: $\alpha + \alpha \leftrightharpoons {}^{8}\mathrm{Be}(n,\gamma)^{9}\mathrm{Be}$

    direct: $\alpha(\alpha n,\gamma)^{9}\mathrm{Be}$
  - reaction rate of ^{9}Be formation is sensitive to fusion mechanism

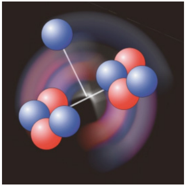

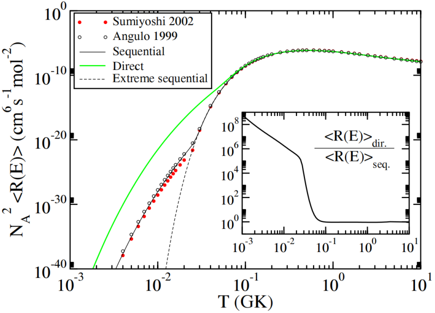

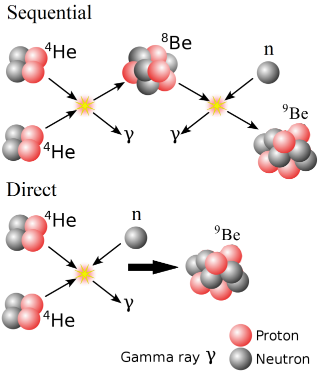

Garrido, et al., EPJA 47 (2011) 102

^{9}Be photodisintegration

- direct measurement of ^{9}Be formation: difficult
- indirect measurement: photodisintegration (inverse process)
  - $1/2+$ resonance: difficult to separate two- and three-body breakup
  - $1/2+$ resonance is close to ^{8}Be resonance
  - requires accurate theoretical analysis

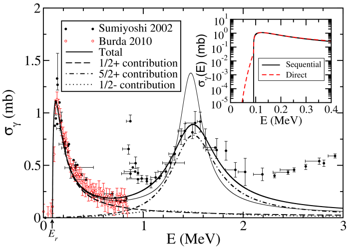

Garrido, et al., EPJA 47 (2011) 102

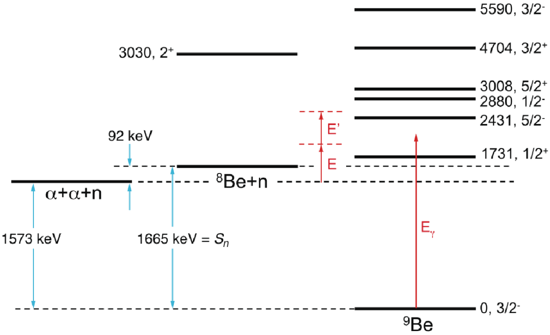

^{9}Be photodisintegration in Halo EFT at NLO

- construct α-α and n-α interaction from halo EFT
- calculate $\alpha\alpha n$ quantumm three-body problem:
  - $\rightarrow$ hyperspherical harmonics expansion
- calculate photoabsorption cross section
  - $\rightarrow$ Lorentz integral transform continuum $\rightarrow$ bound-state

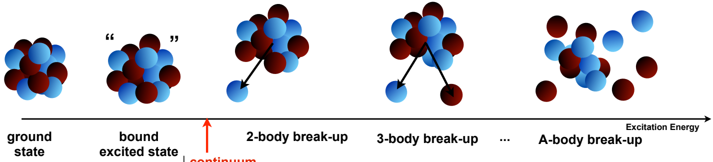

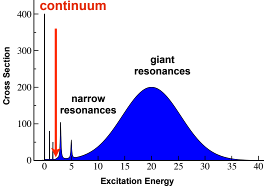

$$\sigma \propto \left|\langle \Psi_f | J^\mu | \Psi_0 \rangle\right|^2$$

Exact knowledge limited in energy and mass number

Capitani, Filandri, CJ, Orlandini, Leidemann

^{9}Be photodisintegration in Halo EFT

- B_3 of ^{9}Be converges when expanding the model space

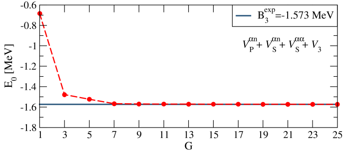

- EFT calculation of photo-disintegration cross section

$\vec{J}_{c,1b}$ only

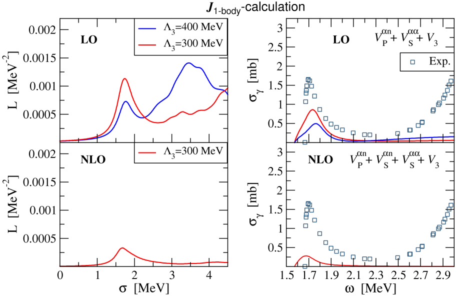

Siegert theorem on $E1$

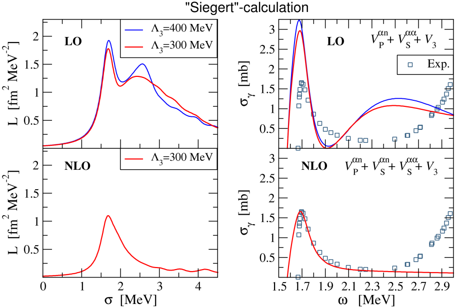

See Ylenia Capitani's Poster

Proton radius and related experiments

- The proton radius puzzle has motivated many new experiments

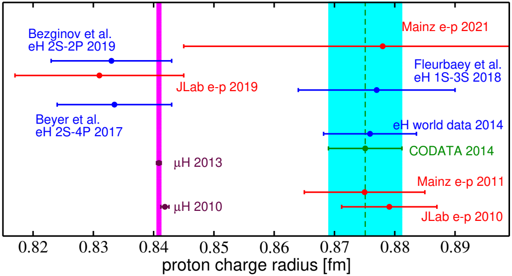

- proton radius
  - ep scattering (JLab, Mainz, Tohoku U.)
  - μp scattering (PSI-MUSE)
  - H spectroscopy (MPQ, LKB, York U.)
  - hyperfine splitting in μH (PSI, RIKEN)
- nuclear radius
  - Lamb shift in $\mu^2\mathrm{H}$, $\mu^{3,4}\mathrm{He}^+$ (PSI-CREMA)
  - hyperfine splitting in $\mu^2\mathrm{H}$, $\mu^3\mathrm{He}^+$ (PSI-CREMA)

Talks by Antognigi, Gao, Meißner

Two-photon exchange contributions to Lamb shift

- Lamb shift & Nuclear structure

$$\delta E_{\rm LS} = \delta_{\rm QED} + \mathcal{A}_{\rm OPE}\, R_E^2 + \delta_{\rm TPE}$$

- $\delta_{\rm TPE} \Longrightarrow$ two-photon contributions

  elastic: Zemach moment $\delta_{\rm Zem}$

  inelastic: polarizability $\delta_{\rm pol}$

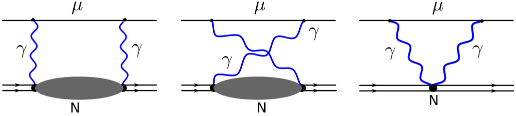

$$\delta_{\rm pol} = \sum_{g,\, S_{\hat{O}}} \int_{\omega_{th}}^{\infty} d\omega\ g\,(\omega)\, S_{\hat{O}}\,(\omega)$$

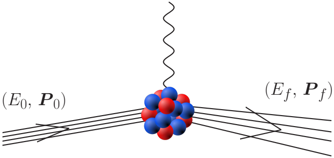

- χEFT + EIHH calculations

CJ, Nevo-Dinur, Bacca, Barnea, PRL 111 (2013) 143402

Hernandez, CJ, Bacca, Nevo-Dinur, Barnea, PLB 736 (2014) 344

Nevo Dinur, CJ, Bacca, Barnea, PLB 755 (2016) 380

Hernandez, Ekström, Nevo Dinur, CJ, Bacca, Barnea, PLB 788 (2018) 377

CJ, Bacca, Barnea, Hernandez, Nevo-Dinur, JPG 45 (2018) 093002

TPE calculation within Pionless EFT framework

- Simple interactions
- Few input parameters: a_t, r_t at NNLO (5% accuracy)

$$\mathcal{L} = N^\dagger \left[i\partial_0 + \frac{\nabla^2}{2M} \right] N - C_0 \left(N^T P_i N\right)^\dagger \left(N^T P_i N\right)$$
$$+ \frac{C_2}{8} \left[\left(N^T P_i N\right)^\dagger \left(N^T \overleftrightarrow{\nabla}^2 P_i N\right) + h.c. \right] - \frac{C_4}{16} \left(N^T \overleftrightarrow{\nabla}^2 P_i N\right)^\dagger \left(N^T \overleftrightarrow{\nabla}^2 P_i N\right)$$

Kaplan, Savage, Wise, Nuclear Physics B 534 (1998) 329

- order-by-order calculation of np scattering t-matrix $\mathcal{A}_n$

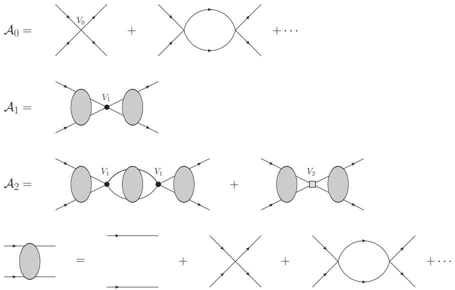

$$C_{0,-1} = -\frac{4\pi}{m_N}\frac{1}{(\mu-\gamma)}, \qquad C_{2,-2} = \frac{2\pi}{m_N}\frac{\rho_d}{(\mu-\gamma)^2},$$
$$C_{0,0} = \frac{2\pi}{m_N}\frac{\rho_d\gamma^2}{(\mu-\gamma)^2}, \qquad C_{2,-1} = -\frac{2\pi}{m_N}\frac{\rho_d^2\gamma^2}{(\mu-\gamma)^3},$$
$$C_{0,1} = -\frac{\pi}{m_N}\frac{\rho_d^2\gamma^4}{(\mu-\gamma)^3}, \qquad C_{4,-3} = -\frac{\pi}{m_N}\frac{\rho_d^2}{(\mu-\gamma)^3},$$

Longitudinal polarizability & Lamb shift in μ^2H

- Longitudinal polarization dominates in $\delta_{\rm pol}$ correction to Lamb shift

  $$\delta_{\rm pol} \propto \iint \mathrm{d}q\, \mathrm{d}\omega\, g(\omega, q) S_{\rm L}(\omega, q)$$

- Longitudinal response function $S_L(\omega, q)$ in $\not{\pi}$EFT

$S_L(\omega, q)$ (LO):

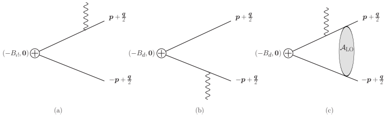

$S_L(\omega, q)$ (NLO):

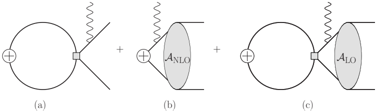

$S_L(\omega, q)$ (N2LO):

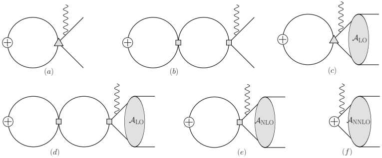

Emmons, CJ*, Platter, J. Phys. G 48, 035101 (2021)

Longitudinal polarizability & Lamb shift in μ^2H

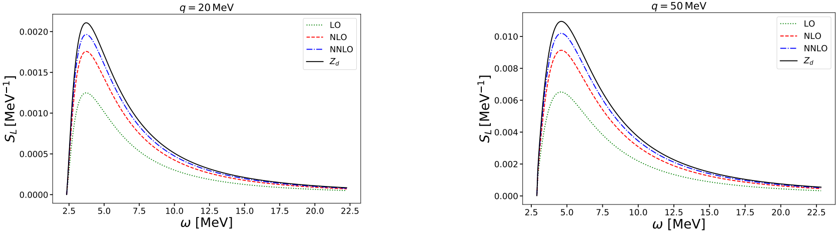

- response functions display an order-by-order convergence in $\pi\!\!\!/$EFT
- $\delta_{\rm pol}$ at NNLO in $\pi\!\!\!/$EFT is consistent with calculations using χEFT interactions

$\delta_{\rm pol}$	NR kernel	R kernel
$\pi\!\!\!/$EFT	-1.605	-1.574
χEFT	-1.590	-1.560

Emmons, CJ*, Platter, J. Phys. G 48, 035101 (2021)

$\delta_{\rm pol}$ at N^{3}LO in $\pi\!\!\!/$EFT:
Lensky, Hagelstein, Pascalutsa,

PLB 835 (2022) 137500; EPJA 58 (2022) 224

TPE contribution to hyperfine splittings in e^{2}H and μ^2H

- Theory prediction of TPE corrections to HFS in e^2H agrees with $\nu_{\rm exp} - \nu_{\rm QED}$
- Theory prediction of TPE corrections to HFS in μ^2H disagrees with $\nu_{\rm exp} - \nu_{\rm QED}$

e^2H 1S $E_{HFS}(2\gamma)$ [kHz]	
$\nu_{\rm exp} - \nu_{\rm qed}$	45 [1]
Faustov 2004	-47
Khriplovich 2004	50
Friar 2005	46

μ^2H 2S $E_{HFS}(2\gamma)$ [meV]	
$\nu_{\rm exp} - \nu_{\rm qed}$	0.0966(73) [2]
Kalinowski 2018	0.0383

[1] Wineland, Ramsey, PRA (1972)
[2] Pohl et al., Science (2016)

TPE effects on HFS in $\not\pi\mathrm{EFT}$

- response functions involved

$$S_0(\omega, q) = \frac{1}{q^2} \mathrm{Im} \sum\!\!\!\!\!\!\!\int_{N \neq N_0} \int \frac{d\hat{q}}{4\pi} \langle N_0 II | \left[\vec{q} \times \vec{J}_m^\dagger(\vec{q}) \right]_3 | N \rangle \langle N | \rho(\vec{q}) | N_0 II \rangle \delta(\omega - \omega_N)$$

$$S_1(\omega, q) = \mathrm{Im} \sum\!\!\!\!\!\!\!\int_{N \neq N_0} \int \frac{d\hat{q}}{4\pi} \epsilon^{3jk} \langle N_0 II | \vec{J}_{m,j}^\dagger(\vec{q}) | N \rangle \langle N | \vec{J}_{c,k}(\vec{q}) | N_0 II \rangle | N_0 II \rangle \delta(\omega - \omega_N)$$

- ρ_E, $\vec{J}_c$, $\vec{J}_m$ all contribute to this problem

$S_{0,1}(\omega, q)$ (LO):

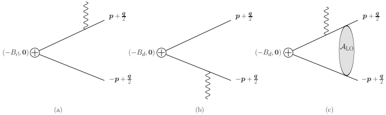

$S_{0,1}(\omega, q)$ (NLO):

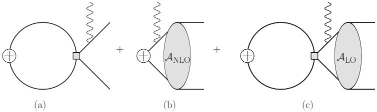

$S_{0,1}(\omega, q)$ (N2LO):

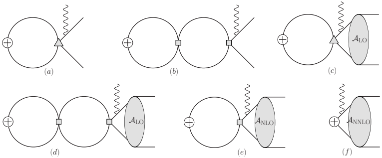

TPE effects on HFS in $\not{\pi}\mathrm{EFT}$

- two-nucleon current in $\not{\pi}\mathrm{EFT}$

$$\mathcal{L}_{2,B} = -ieL_2\epsilon_{ijk}\left(N^T P_i N\right)^\dagger \left(N^T P_j N\right) B_k + \text{h.c.}$$

$S_{0,1}(\omega, q)$ (NLO):

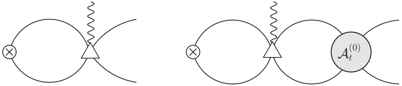

- np S-D mixing (N2LO)

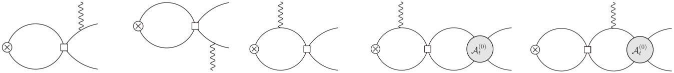

CJ, Zhang, Platter, in progress

$S_0(\omega, q)$ in $\not\pi$EFT

- $S_0(\omega, q)$ display order-by-order convergence

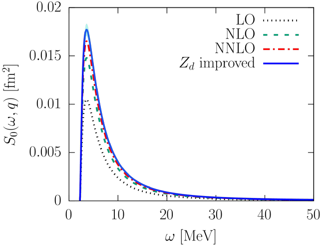

(a) $q = 5$ MeV

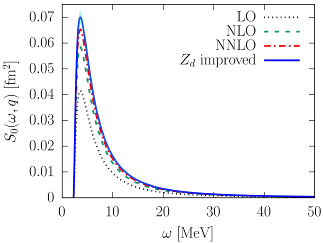

(b) $q = 10$ MeV

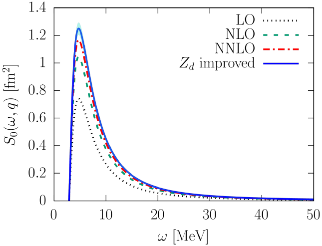

(c) $q = 50$ MeV

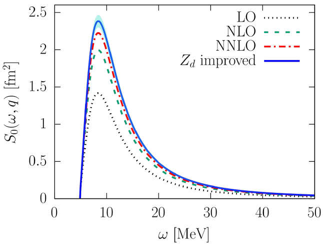

(d) $q = 100$ MeV

$S_0(\omega, q)$ in $\not\pi$EFT

- $S_0(\omega, q)$ is dominated by the iso-vector part ($E1 \times M2$ transition)
- introduce a "conceptual" transition form factor

$$T_0(q) = \int d\omega S_0(\omega, q)$$

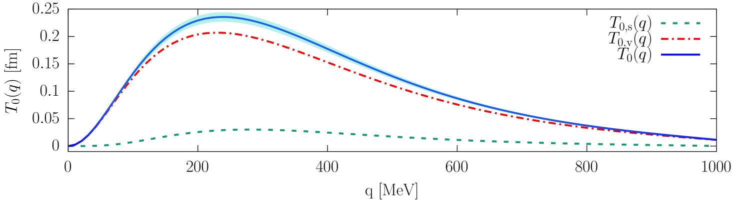

CJ, Zhang, Platter, in progress

Extending to χEFT: Thomas Richardson's talk

Summary

- Effective field theory comes with limited powers determined by Q and Λ, different EFTs are efficient at different energy regimes
- Development of Pionless EFT and Halo EFT provides many tools to tackle low-energy few-body structure and reaction physics
- Halo EFT
  - describes near-threshold physics in a controlled expansion of Q/Λ
  - rejuvenates cluster models with a systematic uncertainty estimates
  - can be combined with *ab initio* calculations
  - helps to understand nucleosynthesis in astrophysical processes
- Pionless EFT
  - provides accurate description of low-energy physics ($Q \ll m_\pi$) in few-nucleon systems
  - is extended to study nuclear structure effects to atomic spectrum, which is crucial for the determination of nuclear radii